Phase signal coupling induced n:m phase synchronization in drive-response oscillators

J. Y. Chen,[1] K. W. Wong,[1] H. Y. Zheng,[2] and J. W. Shuai[3]

[1]*Department of Electronic Engineering, City University of Hong Kong, Hong Kong, China*
[2]*Department of Electronic Engineering, Xiamen University, China*
[3]*Department of Biomedical Engineering, Case Western Reserve University, Cleveland, Ohio 44106*

We have studied phase synchronization between two identical Rössler oscillators connected in the drive-response configuration by a single phase signal. Before the transition to phase synchronization, the distribution of the time interval between consecutive 2π jumps shows several sharp peaks. With a strong phase signal coupling, the n:m phase synchronization between the oscillators can be achieved. For the $n \neq m$ phase synchronizing state, some values of coupling strength result in a phenomenon characterized by a reduction in the mean amplitude of the response termed amplitude reduction. In these regions, the mean rotation speed of the response remains approximately constant while the locking ratio n:m varies.

An interesting phenomenon of practical importance in coupled chaotic oscillators is the synchronizing state [1]. It has been studied extensively in the context of laser dynamics [2], electronic circuits [3], chemical and biological systems [4], and secure communication [5]. Various types of synchronization including complete synchronization [6], lag synchronization [7], and phase synchronization [8] have been studied. It is shown that, for two nonidentical chaotic oscillators with mutual coupling of variables, phase synchronization (PS) can be typically obtained. The coupling variables in these studied PS systems [8] are directly related to the amplitude of the oscillators. Therefore, after PS is obtained at a certain coupling strength, a further increase in the coupling may lead to lag synchronization and complete synchronization [7]. The amplitudes of the two PS systems still have some correlation due to the interacting variables [9]. PS is distinguished from complete synchronization by the appearance of entrainment between the phases of interacting systems with less correlation in signal amplitudes [10]. PS with a 1:1 locking ratio has been widely discussed for coupled Rössler oscillators. An interesting question is in what case can the n:m PS state be observed in coupled Rössler oscillators. It has been shown that chaotic synchronization has important uses for the application of secure communication [5]. In this case, a unidirectional coupling signal is required to be a transferable signal. Thus in order to use PS for secure communication, it is important to find effective methods to achieve PS between two unidirectionally coupled drive-response oscillators.

In this paper, we introduce a method to obtain the n:m PS between two unidirectionally coupled oscillators in which a phase signal is used as the driving force. The system studied in the paper consists of two Rössler oscillators in a drive-response configuration. Its dynamical features of n:m PS are discussed in detail. For the non–phase-locking case, the distribution of the time interval between consecutive 2π jumps shows several peaks. For the n:m PS state with $n \neq m$, the mean amplitude of the response fluctuates substantially when compared with that without any coupling. In a certain range of coupling strength, the mean amplitude could become very small. This is referred to as the amplitude reduction phenom-

enon. At the transition for various n:m PS states, a linear relationship between the mean amplitude and the n:m ratio is found in the amplitude reduction region. Our simulations further show that the mean rotation speed of the response oscillator is maintained approximately constant throughout transitions to various n:m PS states. As the phenomena of amplitude death and semideath in two coupled nonlinear oscillators and their possible application in physics, chemistry, medicine, and biology have been observed and studied [11], the investigation of amplitude reduction may also lead to potential application in those areas.

The proposed phase-driven method is first illustrated using two identical Rössler oscillators configured in the drive-response mode. A general n:m PS can be found for the response oscillator driven by a single phase signal from the driver. The drive oscillator is described by the following set of equations [12]:

$$\dot{x}_1 = -y_1 - z_1,$$

$$\dot{y}_1 = x_1 + 0.15 y_1, \qquad (1)$$

$$\dot{z}_1 = 0.2 + z_1(x_1 - 10).$$

The response oscillator is governed by

$$\dot{x}_2 = -y_2 - z_2 + \varepsilon(r_2 \cos(\beta \phi_1) - x_2),$$

$$\dot{y}_2 = x_2 + 0.15 y_2 + \varepsilon(r_2 \sin(\beta \phi_1) - y_2), \qquad (2)$$

$$\dot{z}_2 = 0.2 + z_2(x_2 - 10),$$

where ϕ_1 is the phase of the driver, r_2 is the amplitude of the response system, and ε is the coupling strength. The parameter β is given by n/m, which is termed the locking ratio. The phase and the amplitude of the Rössler attractor are, respectively, defined as [13]

$$\phi_i = \arctan\left(\frac{y_i}{x_i}\right) \quad \text{with} \ i = 1,2, \qquad (3)$$

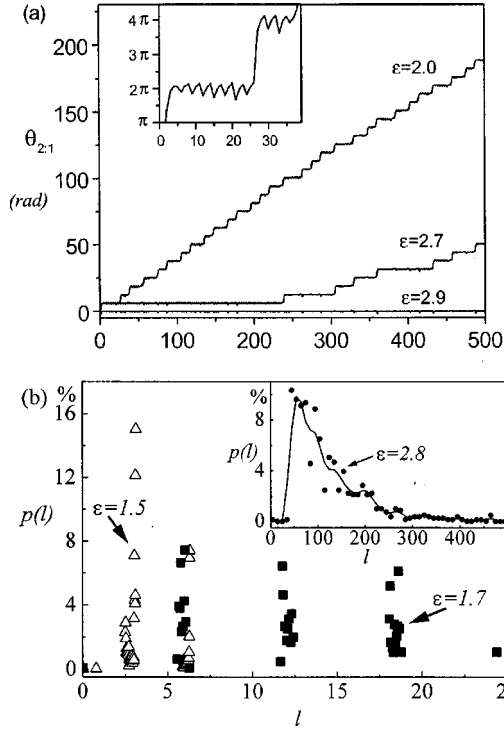$$r_i = (x_i^2 + y_i^2)^{1/2} \quad \text{with} \ i = 1,2. \qquad (4)$$

FIG. 1. Phase jump phenomena in a system composed of two Rössler oscillations at various coupling strengths. The phase locking ratio is $n:m=2:1$. (a) Time evolution of the phase separation $\theta_{n:m}$. The inset shows a single 2π jump enlarged from the curve for $\varepsilon=2.0$. (b) Probability distribution function $p(l)$ of the time interval l between two adjacent 2π jumps. The open triangles indicate the distribution at $\varepsilon=1.5$. The solid squares show the distribution at $\varepsilon=1.7$. The distribution in the inner plot is for $\varepsilon=2.8$.

The $n:m$ phase-locking condition requires

$$|\theta_{n:m}(t)| < \text{const}, \qquad (5)$$

where $\theta_{n:m}(t)=n\phi_1(t)-m\phi_2(t)$ is the generalized phase separation or the relative phase. Note that both the phase and the phase separation are defined on the whole real line, rather than in the region of $[0,2\pi]$. The locking condition specified by Eq. (5) is equivalent to frequency locking, i.e., $n\Omega_1 = m\Omega_2$, where $\Omega_i = \langle \dot{\phi}_i \rangle$ with $i=1,2$ [14]. With the mean frequency, the mean frequency difference is defined,

$$\Delta\Omega_{n:m}=n\Omega_1-m\Omega_2. \qquad (6)$$

Equations (2) and (5) indicate that the amplitudes of the two oscillators are not directly correlated since the driving signal is the phase signal of the drive oscillator.

We perform simulations with $n:m=2:1$. That is, the frequency of the response oscillator is twice the intrinsic frequency of the drive oscillator. All simulations reported omit the first 1×10^3 units of time. Curves of the phase separation versus time are plotted in Fig. 1(a) for coupling strengths $\varepsilon =2.9$, 2.7, and 2.0. The transition to 2:1 PS occurs at $\varepsilon =2.89\pm0.005$. This value of the coupling strength is referred to as the critical coupling strength $\varepsilon_{2:1}^c$. The uncertainty is mainly caused by the fact that in all our simulations,
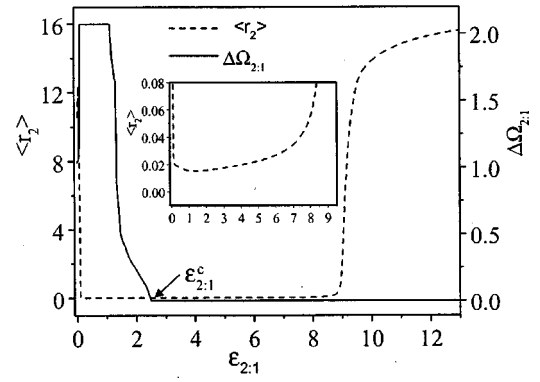

FIG. 2. The mean amplitude $\langle r_2 \rangle$ and the corresponding frequency difference $\Delta\Omega_{2:1}$ at coupling strength $0<\varepsilon_{2:1}<13$. The left vertical axis is for the $\langle r_2\rangle - \varepsilon_{2:1}$ plane while the right one corresponds to the $\Delta\Omega_{2:1}-\varepsilon_{2:1}$ plane. The region where $\langle r_2\rangle$ is close to zero corresponds to amplitude reduction. The inner plot is an enlargement of this amplitude reduction region. $\varepsilon_{2:1}^c$ is the critical coupling strength at the transition to PS.

the step size of the coupling strength is chosen as 0.01. When $\varepsilon<\varepsilon_{2:1}^c$, the phase separation $\theta_{2:1}$ increases progressively by 2π jumps, as shown in the inset of Fig. 1(a). If $\varepsilon \geq \varepsilon_{2:1}^c$, the phase separation is basically zero with a small high-frequency fluctuation. The corresponding mean frequency difference is shown on the $\Delta\Omega_{2:1}-\varepsilon_{2:1}$ plane in Fig. 2. When the coupling strength increases from zero, the mean frequency difference reduces continuously. After the transition point, we have $\Delta\Omega_{2:1}\to0$.

In order to quantify the dynamics of phase separation near and away from the PS transition in Fig. 1(a), we compute the probability distribution function $p(l)$ of the time interval l between two successive 2π jumps for various values of coupling strength. It is plotted in Fig. 1(b) for $\varepsilon=1.5$, 1.7, and 2.8. For $\varepsilon=1.5$, shown with an open triangle, there are only two clusters for the distribution function at the time intervals of 3.1 and 6.3. Therefore, the distribution of time intervals between consecutive 2π jumps for $\varepsilon=1.5$ could be considered as having only two sharp peaks. When $\varepsilon=1.7$, the solid squares show three main peaks of time interval at 5.9, 12.0, and 18.4. The difference between two adjacent peaks is nearly equal to 6. However, with a further increase of coupling strength, the bandwidth enlarges and the peak location becomes ambiguous. When the coupling strength is close to the critical transition value, the statistics follow a Lorentzian curve [13] whose distribution function is asymmetrical. This is shown in the inner plot of Fig. 1(b).

A peaked distribution for the time interval between consecutive 2π phase jumps could be found at various values of β, except for $\beta=1$. When the coupling strength moves away from the critical value $\varepsilon_{n:m}^c$, the distribution $p(l)$ changes from a Lorentzian curve to sharp peaks. The corresponding bandwidth narrows. Some researchers have reported that at a certain coupling strength, the phase separation increases with a nearly periodic sequence of 2π jumps [13]. However, the phase jump phenomena observed here occur at several values of time interval. This is due to the fact that the former PS phenomenon is caused by two nonidentical coupled oscilla-
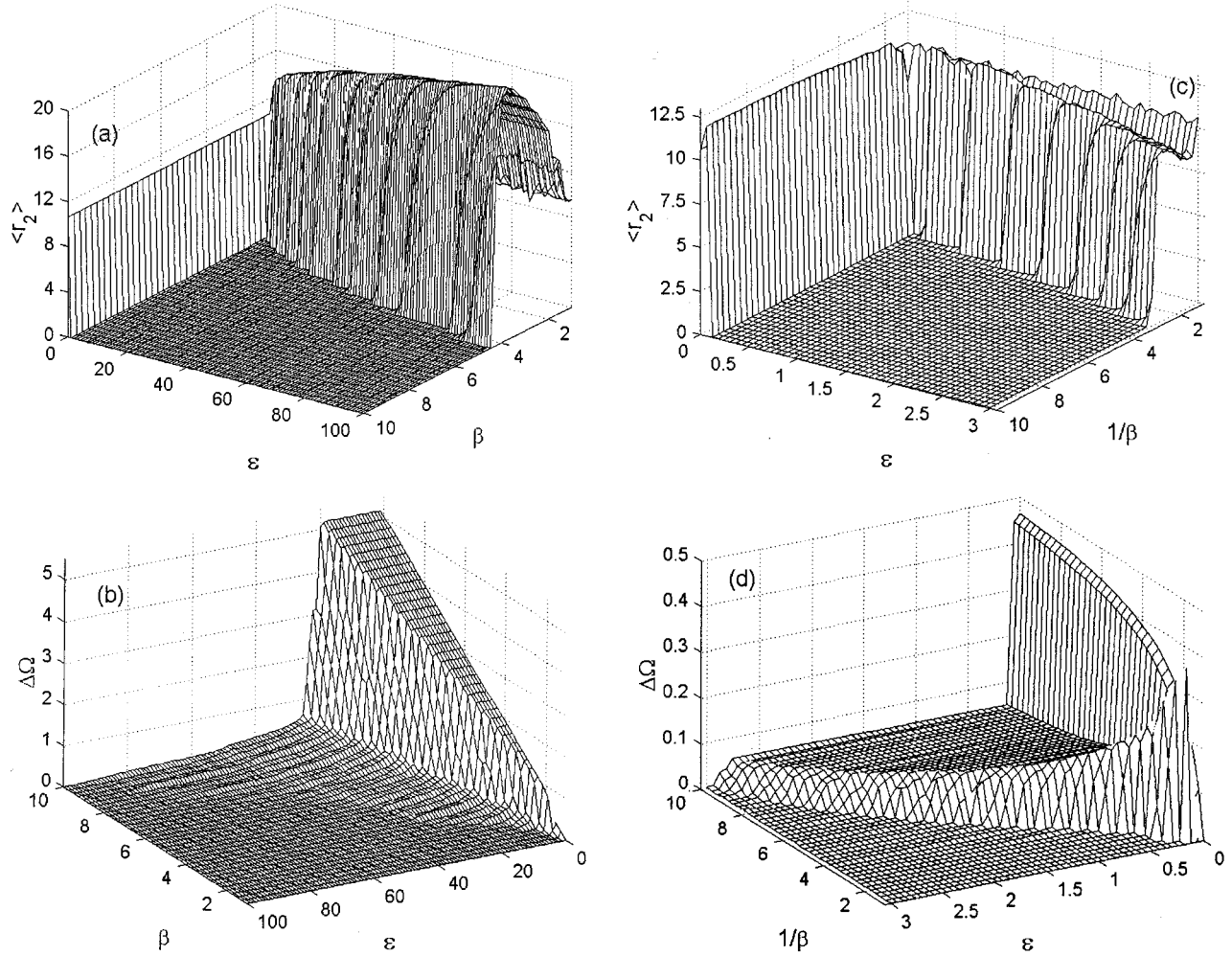
FIG. 3. (a)–(d) The mean amplitude $\langle r_2 \rangle$ and the mean frequency difference $\Delta\Omega$ vs the coupling strength ε and the locking ratios β or $1/\beta$ in the response oscillators. In (a) and (b), simulations are taken with β from 1 to 10 at the interval of 0.25 and ε from 0 to 100 at the interval of 1. In (c) and (d), simulations are taken with $1/\beta$ from 1 to 10 at the interval of 0.25 and ε from 0 to 3 at the interval of 0.06.

tors running at the same frequency while the PS studied here is based on two identical drive-response oscillators at different frequency.

When $n \neq m$, an increase of coupling strength can cause the mean amplitude to be reduced substantially. However, this amplitude reduction phenomenon occurs only in a certain region. A further increase of coupling strength causes the mean amplitude to be enlarged. In order to investigate this feature in detail, we calculate the mean amplitude $\langle r_2 \rangle$ of the response oscillator. Note that the mean amplitude of the drive oscillator is $\langle r_1 \rangle = 10.65$, which is the same as that of the response when $\varepsilon = 0$.

The locking ratio remains n:$m = 2$:1 and the simulation is performed in the coupling range $0 < \varepsilon_{2:1} < 13$. The corresponding mean amplitude $\langle r_2 \rangle$ is also plotted in Fig. 2. As coupling strength is increased from zero, the mean amplitude rapidly shrinks. However, the mean frequency difference $\Delta\Omega_{2:1}$ does not decrease to zero until the coupling strength exceeds the PS critical value, i.e., $\varepsilon_{2:1} \geq \varepsilon^c_{2:1}$. In the phase-locking region $2.9 < \varepsilon_{2:1} < 9$, the mean amplitude remains low, as shown in Fig. 2. When $\varepsilon_{2:1} > 9$, the mean amplitude

of the response jumps up rapidly and at last exceeds that of the drive oscillator. Within the amplitude reduction region, the mean amplitude rises, but at a relatively slow rate when compared with the rapid jump at $\varepsilon_{2:1} > 9$. This is illustrated by the inner plot of Fig. 2.

Amplitude reduction is a general phenomenon at various locking ratios except n:$m = 1$:1, as shown in Figs. 3(a)–3(d). Figures 3(a) and 3(b) show, respectively, the distribution of the mean amplitude and the corresponding mean frequency difference for β from 1 to 10 and ε from 0 to 100. When $\beta = 1$, the mean amplitude of the response oscillator never shrinks, even at large coupling strength. For increased β, the region of coupling strength where amplitude reduction is observed also enlarges. When $\beta > 5.5$, the mean amplitude remains shrunk even at $\varepsilon = 100$. The corresponding mean frequency difference is shown in Fig. 3(b). Note the change in the view angle of Figs. 3(a) and 3(b). In Fig. 3(b), PS is always achieved with any coupling strength when $\beta = 1$. Three distinct regions can be identified. With a small coupling, the increase of β causes a linear increase of $\Delta\Omega$ in the range $\Delta\Omega > 1$. This is because under a small coupling

strength, $\Omega_1 \approx \Omega_2$. The approximately linear relationship between β and $\Delta\Omega$ could be found from Eq. (6). On the other hand, PS is observed with a large coupling strength. Between these two regions, there is a non–phase-locking region with small $\Delta\Omega$ (<0.5). It is observed from the figure that to get phase locking for a larger β, a larger ε is needed. Recent investigation of PS always relates to weak coupling [8]. However, in our study, strong coupling can also lead to PS. For example, when $\varepsilon = 100$, we observe from Fig. 3(a) that $\langle r_2 \rangle \neq \langle r_1 \rangle$. But Fig. 3(b) shows that the mean frequency difference is zero in the corresponding region. Therefore, PS is obtained with β from 1 to 10 when $\varepsilon = 100$.

Similar phenomena can be found when the frequency of the response oscillator is lower than that of the driver. Figures 3(c) and 3(d) show the distribution of the mean amplitude and the corresponding mean frequency difference with $1/\beta$ from 1 to 10 and ε from 0 to 3. However, there are some differences when compared with Figs. 3(a) and 3(b). With the increase of coupling strength, $\langle r_2 \rangle$ jumps up from the amplitude reduction region and its value seen in Fig. 3(c) is always less than that of the drive oscillator. On the contrary, Fig. 3(a) shows that this value is always larger than that of the driver under the same situation.

In the nonsynchronous region of Fig. 3(d), as $1/\beta$ increases, the mean frequency difference increases at $\varepsilon \approx 0$ and decreases when $\varepsilon > 0$. However, in the same region of Fig. 3(b), an increase of β results in an increase of $\Delta\Omega$ at various ε. In our simulation, PS is always found for $1/\beta$ from 1 to 10 when $\varepsilon > 3$. However, in Fig. 3(b), this phenomenon is only observed when $\varepsilon > 90$. In this regard, Fig. 3(d) only shows the mean frequency difference corresponding to ε from 0 to 3.

It is interesting to extract additional information about the relationship between $\langle r_2 \rangle$ and β in the amplitude reduction region. Further simulations are performed with the locking ratio varied in the range $5 \leq \beta$ (or $1/\beta$) ≤ 10. The obtained data are plotted in Fig. 4(a). All the mean amplitudes are obtained in the PS region with coupling strengths equal to $1.0\varepsilon_{n:m}^c$, $1.4\varepsilon_{n:m}^c$, $1.8\varepsilon_{n:m}^c$, and $2.0\varepsilon_{n:m}^c$, respectively. For $\beta > 1$, the four solid curves show an inversely proportional relationship between $\langle r_2 \rangle$ and β. The change in the slope of the curves follows the same trend for the four coupling strengths considered. For $\beta < 1$, the dotted lines also indicate the same inversely proportional relationship [note that in Fig. 4(a), the horizontal coordinate is $1/\beta$ when $\beta < 1$]. However, an increase of coupling strength results in a change of the slope of the dotted lines. When the coupling strength is far away from the PS critical value, e.g., $\varepsilon_{n:m} = 2.0\varepsilon_{n:m}^c$ and $1/\beta > 7.5$, the corresponding dotted line jumps up rapidly. This indicates that $\langle r_2 \rangle$ has jumped out of the amplitude reduction region because of the large coupling strength. Similarly, a further increase of coupling strength for $\beta > 1$ could also cause $\langle r_2 \rangle$ to jump out of the amplitude reduction region (not shown). On the other hand, when the coupling strength is close to the critical value, e.g., at $1.0\varepsilon_{n:m}^c$ and $1.4\varepsilon_{n:m}^c$, the slope of the dotted lines is approximately constant when $5 < 1/\beta < 10$. The solid lines show the inversely proportional relationship when $5 < \beta < 10$.
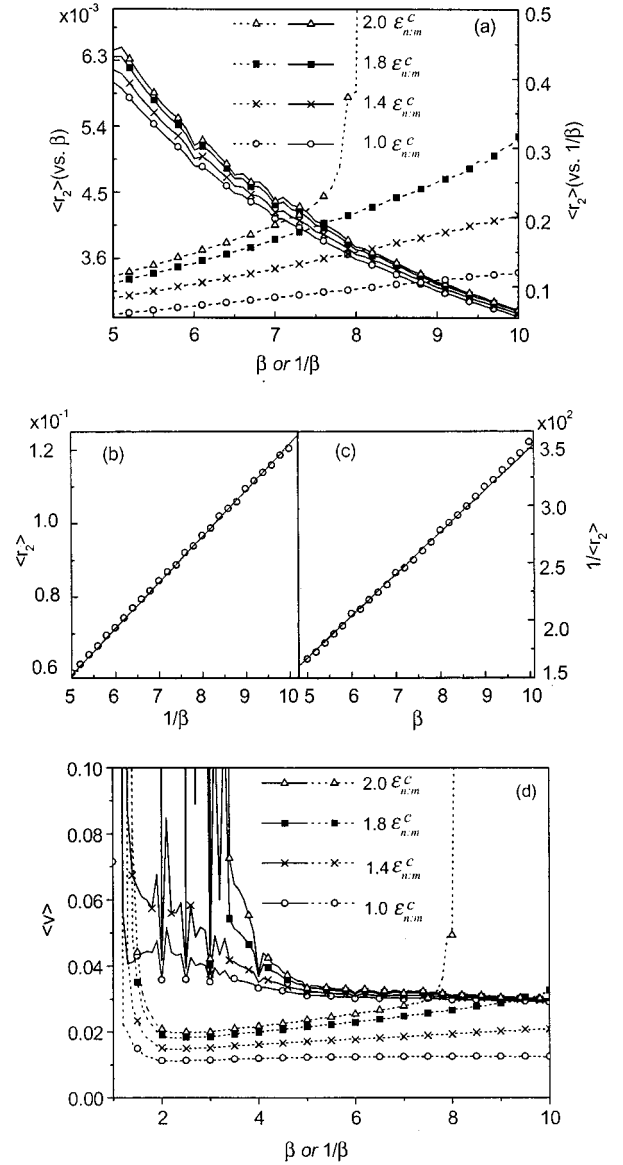

FIG. 4. (a) The mean amplitude $\langle r_2 \rangle$ at various locking ratios and coupling strengths. The left vertical coordinate is for the $\langle r_2 \rangle$-β plane while the right one corresponds to $\langle r_2 \rangle$-$1/\beta$. (b) The relationship between $\langle r_2 \rangle$ and $1/\beta$. (c) The relationship between $1/\langle r_2 \rangle$ and β at various locking ratios with $\varepsilon_{n:m} = 1.0\varepsilon_{n:m}^c$, where $\varepsilon_{n:m}^c$ is the coupling strength at transition for locking ratio $n:m$. The open circles correspond to the data obtained in simulation while the lines are resulted from linear fitting. (d) The mean rotation speed $\langle \nu \rangle$ at various locking ratios and coupling strengths. In (a) and (d), the solid lines correspond to $\beta > 1$ while the dotted lines correspond to $\beta < 1$. When $\beta < 1$, the horizontal coordinate is written as $1/\beta$.

In the following, we investigate further the slope coefficient of $\langle r_2 \rangle$ versus β (or $1/\beta$) in the amplitude reduction region. We perform linear line fitting for the solid and dotted lines corresponding to $\varepsilon_{n:m} = 1.0\varepsilon_{n:m}^c$ in Fig. 4(a) and plot the results in Figs. 4(b) and 4(c), respectively. In order to show the relationship clearly, the latter graph is plotted as $1/\langle r_2 \rangle$ versus β. In Fig. 4(b), an empirical formula $\langle r_2 \rangle = \kappa^-(1/\beta) + \rho^-$ is used while it is $1/\langle r_2 \rangle = \kappa^+\beta + \rho^+$ for Fig. 4(c). In

the formula, κ^- and κ^+ are the slope coefficients while ρ^- and ρ^+ represent the intercepts. The results of line fitting show that $\kappa^- = 1.3 \times 10^{-2}$, $\rho^- = 3.8 \times 10^{-3}$, $\kappa^+ = 36.5$, and $\rho^+ = -14.9$. As a result, we may assume that the relationship between $\langle r_2 \rangle$ and β can be described by the assumed empirical formula. In this regard, one can find that the mean amplitude and the locking ratio have a linear relationship when the locking ratio is far away from $n:m = 1:1$ and the coupling strength is near the critical value for transition to PS.

For a rotational movement, the speed of rotation can be defined. In particular, the mean rotation speed of the chaotic response oscillator can be expressed as

$$\langle \nu \rangle = \langle r_2 \rangle \Omega_2. \tag{7}$$

Simulation results of the mean rotation speed versus phase-locking ratio β for the four coupling strengths studied above are shown in Fig. 4(d). The solid lines correspond to the $\langle \nu \rangle$-β plane with $\beta > 1$ while the dotted lines are on the $\langle \nu \rangle$-$1/\beta$ plane with $\beta < 1$. For $\beta > 1$, the increase of β at first causes a reduction of the mean rotation speed. This speed then remains almost constant even when the coupling strength varies from $1.0\varepsilon_{n:m}^c$ to $2.0\varepsilon_{n:m}^c$. However, a smaller β is sufficient to approach constant rotation speed when the coupling strength is close to the transition coupling. For $\beta < 1$, an increase of $1/\beta$ from 1 to 2 causes a sharp reduction of the mean rotation speed. A nearly constant mean rotation speed is observed in the range $\beta < 0.5$, i.e., $1/\beta > 2$, when the coupling is equal to $\varepsilon_{n:m}^c$ or $1.4\varepsilon_{n:m}^c$. For the couplings $\varepsilon_{n:m} = 1.8\varepsilon_{n:m}^c$ and $2.0\varepsilon_{n:m}^c$, the mean rotation speed increases when $1/\beta$ increases from 2.

In fact, the behavior of $\langle \nu \rangle$ versus β is closely related to the behavior of $\langle r_2 \rangle$ versus β, as governed by Eq. (7). It is the linear relationship between $\langle r_2 \rangle$ and β that has led to the constant mean rotation speed. For example, considering $\Omega_2 = (n/m)\Omega_1 = \beta\Omega_1$ and $\beta > 5$, we have $1/\langle r_2 \rangle = \kappa^+ \beta + \rho^+$. Then Eq. (7) can be rewritten as

$$\langle \nu \rangle = \frac{\beta\Omega_1}{\kappa^+ \beta + \rho^+}. \tag{8}$$

For $\beta > 5$, $\kappa^+ \beta \gg \rho^+$. Therefore, we have $\langle \nu \rangle \approx \Omega_1 / \kappa^+$. Similarly, we have $\langle \nu \rangle \approx \kappa^- \Omega_1$ for $1/\beta > 2$. When $1/\beta > 7.5$

and $\varepsilon_{n:m} = 2.0\varepsilon_{n:m}^c$, the mean rotation speed jumps up rapidly as the mean amplitude $\langle r_2 \rangle$ begins to leave the amplitude reduction region shown in Fig. 4(a).

The demonstration of PS in a system driven by a single unidirectional phase signal is important to facilitate the application of PS. This is because the amplitudes of the drive and the response oscillators are shown to have less correlation with each other. Thus an increase of the coupling strength will not drive PS to complete synchronization. Moreover, the proposed phase driving scheme can realize various $n:m$ phase-locking modes as required, and also in various styles of coupling such as two or several nonidentical interacting couplings, etc. Similar to the application of complete synchronization achieved by using a single amplitude signal in secure communication, the proposed scheme also facilitates the application of PS in this field. As the control of a phase signal may also result in the symbolic dynamics following a desired symbol sequence [15], this information-encoding method may be utilized in secure communication by a single unidirectional phase signal. The feature of constant mean rotation speed at various locking ratios may also help in information encoding. Such applications using the phase signal as driver will be investigated in detail.

In conclusion, we have proposed a method to achieve $n:m$ PS in which the drive-response oscillators are connected by only a single unidirectional phase signal. The amplitudes between the oscillators remain uncorrelated with increased coupling strength. The time interval between consecutive 2π jumps typically appears at several intervals when the coupling strength is far from the PS transition point. The response oscillator shows amplitude reduction when $n \neq m$. Simulations show that the mean amplitude in the amplitude reduction region has a linear relationship with the locking ratio. Moreover, the mean rotation speed of the response attractor remains constant throughout the coupling strength near the PS transitions at various locking ratios far away from $n:m = 1:1$. All these features as well as the method of using a single phase signal to obtain phase locking may be utilized in communication.

[1] N. Koppel and G. B. Ermentrout, Commun. Pure Appl. Math. **39**, 623 (1986); P. C. Matthews and S. H. Strogatz, Phys. Rev. Lett. **65**, 1701 (1990); M. D. S. Vieira, A. J. Lichtenberg, and M. A. Lieberman, Int. J. Bifurcation Chaos Appl. Sci. Eng. **4**, 1563 (1994).

[2] L. Fabiny, P. Colet, and R. Roy, Phys. Rev. A **47**, 4287 (1993); R. Roy and K. S. Thornburg, Jr., Phys. Rev. Lett. **72**, 2009 (1994).

[3] J. F. Heagy, T. L. Caroll, and L. M. Pecora, Phys. Rev. E **50**, 1874 (1994); V. S. Anischenko, T. E. Vadivasova, D. E. Postnov, and M. A. Safonova, Int. J. Bifurcation Chaos Appl. Sci. Eng. **2**, 633 (1992).

[4] I. Schreiber and M. Marek, Physica D **5**, 258 (1982); S. K. Han, C. Kurrer, and Y. Kuramoto, Phys. Rev. Lett. **75**, 3190 (1995).

[5] L. Kocarev and U. Parlitz, Phys. Rev. Lett. **74**, 5028 (1995).

[6] J. Y. Chen, K. W. Wong, and J. W. Shuai, Phys. Lett. A **263**, 315 (1999); Z. H. Liu, S. G. Chen, and B. B. Hu, Phys. Rev. E **59**, 2817 (1999); J. H. Peng, E. J. Ding, M. Ding, and W. Yang, Phys. Rev. Lett. **76**, 904 (1996); Y. Liu and P. Davis, Phys. Rev. E **61**, 2176 (2000).

[7] M. G. Rosenblum, A. S. Pikovsky, and J. Kurths, Phys. Rev. Lett. **76**, 1804 (1996).

[8] J. Y. Chen, K. W. Wong, Z. X. Chen, S. C. Xu, and J. W. Shuai, Phys. Rev. E **61**, 2559 (2000); S. Boccaletti, J. Bragrad, F. T. Arecchi, and H. Mancinil, Phys. Rev. Lett. **83**, 536

(1999); D. E. Postnov, A. G. Balanov, N. B. Janson, and E. Mosekilde, *ibid.* **83**, 1942 (1999); V. Andrade, R. L. Davidchack, and Y. C. Lai, Phys. Rev. E **61**, 3230 (2000); D. Hoyer, O. Hoyer, and U. Zwiener, IEEE Trans. Biomed. Eng. **47**, 68 (2000).

[9] J. W. Shuai and D. M. Durand, Phys. Lett. A **264**, 289 (1999).

[10] A. S. Pikovsky, M. G. Rosenblum, G. V. Osipov, and J. Kurths, Physica D **104**, 219 (1997).

[11] R. Herrero, M. Figueras, J. Rius, F. Pi, and G. Orriols, Phys. Rev. Lett. **84**, 5312 (2000); R. C. Elson, A. I. Selverston, R. Huerta, N. F. Rulkov, M. I. Rabinovich, and H. D. I. Abarbanel, *ibid.* **81**, 5692 (1998); S. H. Strogatz, Nature (London) **394**, 316 (1998).

[12] O. E. Rössler, Phys. Lett. **57A**, 397 (1976).

[13] K. J. Lee, Y. Kwak, and T. K. Lim, Phys. Rev. Lett. **81**, 321 (1998); E. Rosa, Jr., E. Ott, and M. H. Hess, *ibid.* **80**, 1642 (1998).

[14] P. Tass, M. G. Rosenblum, J. Weule, J. Kurths, A. Pikovsky, J. Volkmann, A. Schnitzler, and H. J. Freund, Phys. Rev. Lett. **81**, 3291 (1998).

[15] Y. C. Lai, E. Bollt, and C. Grebogi, Phys. Lett. A **255**, 75 (1999); E. Ott, G. Grebogi, and J. A. Yorke, Phys. Rev. Lett. **64**, 1196 (1990); E. Bollt, Y. C. Lai, and C. Grebogi, *ibid.* **79**, 3787 (1997); S. Hayes, C. Grebogi, and E. Ott, *ibid.* **70**, 3031 (1993); S. Hayes, C. Grebogi, E. Ott, and A. Mark, *ibid.* **73**, 1781 (1994); E. Bollt and Y. C. Lai, Phys. Rev. E **58**, 1724 (1998); E. M. Bollt and M. Dolnik, *ibid.* **55**, 6404 (1997).